AFRL-RX-WP-TP-2009-4093

ANISOTROPY OF THE HOT PLASTIC DEFORMATION OF Ti-6Al-4V SINGLE-COLONY SAMPLES (PREPRINT)

A.A. Salem and S.L Semiatin

Metals Branch
Metals, Ceramics and NDE Division

APRIL 2009

AIR FORCE RESEARCH LABORATORY
MATERIALS AND MANUFACTURING DIRECTORATE
WRIGHT-PATTERSON AIR FORCE BASE, OH 45433-7750
AIR FORCE MATERIEL COMMAND
UNITED STATES AIR FORCE

REPORT DOCUMENTATION PAGE

Form Approved
OMB No. 0704-0188

1. REPORT DATE *(DD-MM-YY)*	2. REPORT TYPE	3. DATES COVERED *(From - To)*
April 2009	Journal Article Preprint	01 April 2009- 01 April 2009

4. TITLE AND SUBTITLE
ANISOTROPY OF THE HOT PLASTIC DEFORMATION OF Ti-6Al-4V SINGLE-COLONY SAMPLES (PREPRINT)

5a. CONTRACT NUMBER
In-house

5b. GRANT NUMBER

5c. PROGRAM ELEMENT NUMBER
62102F

6. AUTHOR(S)
A.A. Salem and S.L. Semiatin (AFRL/RXLMP)

5d. PROJECT NUMBER
4347

5e. TASK NUMBER
RG

5f. WORK UNIT NUMBER
M02R2000

7. PERFORMING ORGANIZATION NAME(S) AND ADDRESS(ES)

Metals Branch (RXLMP)
Metals, Ceramics and NDE Division
Materials and Manufacturing Directorate
Wright-Patterson Air Force Base, OH 45433-7750
Air Force Materiel Command, United States Air Force

8. PERFORMING ORGANIZATION REPORT NUMBER
AFRL-RX-WP-TP-2009-4093

9. SPONSORING/MONITORING AGENCY NAME(S) AND ADDRESS(ES)
Air Force Research Laboratory
Materials and Manufacturing Directorate
Wright-Patterson Air Force Base, OH 45433-7750
Air Force Materiel Command
United States Air Force

10. SPONSORING/MONITORING AGENCY ACRONYM(S)
AFRL/RXLMP

11. SPONSORING/MONITORING AGENCY REPORT NUMBER(S)
AFRL-RX-WP-TP-2009-4093

12. DISTRIBUTION/AVAILABILITY STATEMENT
Approved for public release; distribution unlimited.

13. SUPPLEMENTARY NOTES
To be submitted to Materials Science & Engineering A
PAO Case Number and clearance date: 88ABW-2008-1250, 10 December 2008.

14. ABSTRACT
The critical resolved shear stresses and flow curves for the seven possible slip systems in Ti-6Al-4V with a lamellar microstructure were determined via high temperature uniaxial compression testing. For this purpose, samples with a rectangular cross section were cut from single colonies grown using a float-zone technique and then tested at 815°C. Each sample was oriented for single slip along one of seven different slip systems in the alpha phase; i.e., one of the three <1120>{1010} (prism <a>), the three <1120>{0001} (basal <a>), or the <c+a> (pyramidal) systems was activated by orienting specific samples to have the highest Schmid factor on that particular system. Measurements of the critical resolved shear stress (CRSS) at yielding and the subsequent flow behavior revealed a strong dependence of mechanical behavior on colony orientation/activated slip system. The anisotropy in the CRSS and the tendency for flow softening at large strains was rationalized on the basis of the Burgers orientation relationship between the alpha (hcp) lamellae and the beta (bcc) matrix and hence the orientation of alpha slip directions relative to those in the beta phase.

15. SUBJECT TERMS
Deformation mechanisms; Ti-6Al-4V; single colony; critical resolved shear stress; high temperature

16. SECURITY CLASSIFICATION OF:			17. LIMITATION OF ABSTRACT:	18. NUMBER OF PAGES	19a. NAME OF RESPONSIBLE PERSON (Monitor)
a. REPORT	b. ABSTRACT	c. THIS PAGE			Sheldon L. Semiatin
Unclassified	Unclassified	Unclassified	SAR	28	19b. TELEPHONE NUMBER *(Include Area Code)* N/A

Standard Form 298 (Rev. 8-98)
Prescribed by ANSI Std. Z39-18

Anisotropy of the hot plastic deformation of Ti-6Al-4V single-colony samples

A.A. Salem[1,*] and S.L. Semiatin[1]

[1] Air Force Research Laboratory, Materials and Manufacturing Directorate, AFRL/RXLM, Wright-Patterson AFB, OH 45433

Abstract

The critical resolved shear stresses and flow curves for the seven possible slip systems in Ti-6Al-4V with a lamellar microstructure were determined via high temperature uniaxial compression testing. For this purpose, samples with a rectangular cross section were cut from single colonies grown using a float-zone technique and then tested at 815°C. Each sample was oriented for single slip along one of seven different slip systems in the alpha phase; i.e., one of the three $<11\bar{2}0>\{10\bar{1}0\}$ (prism <a>), the three $<11\bar{2}0>\{0001\}$ (basal <a>), or the <*c*+*a*> (pyramidal) systems was activated by orienting specific samples to have the highest Schmid factor on that particular system. Measurements of the critical resolved shear stress (CRSS) at yielding and the subsequent flow behavior revealed a strong dependence of mechanical behavior on colony orientation/activated slip system. The anisotropy in the CRSS and the tendency for flow softening at large strains was rationalized on the basis of the Burgers orientation relationship between the alpha (hcp) lamellae and the beta (bcc) matrix and hence the orientation of alpha slip directions relative to those in the beta phase.

Keywords: Deformation mechanisms; Ti-6Al-4V; single colony; critical resolved shear stress; high temperature

*Corresponding author. Tel:+1-937-255-1314; fax;+1-937-252-6373.
Universal Technology Corp., Dayton, OH 45432; work performed under USAF contract #F33615-03-D-5801.
E-mail address: ayman.salem@wpafb.af.mil (A.A. Salem)

1. Introduction

Providing an excellent combination of high strength, corrosion resistance, and low density, Ti-6Al-4V is the most commonly used alpha/beta titanium alloy. It accounts for approximately 80% of the total titanium used in the US [1].

The mechanical behavior of Ti-6Al-4V depends on the microstructure and texture developed during thermomechanical processing (TMP) [2, 3]. Depending on the specific TMP practice, one of three principal microstructures is commonly formed [2, 3], namely, fully lamellar alpha, fully equiaxed alpha, and bi-modal (duplex). The fully lamellar and bi-modal microstructures both have lamellae of hcp alpha (α) phase in a matrix of bcc beta (β) phase. The fully lamellar microstructure is formed during cooling from the beta field at a slow-to-medium rate; the lamellar-alpha phase and the beta matrix in which it grows follow a Burgers orientation relationship (OR) in which $(0001)_\alpha$ is parallel to $(101)_\beta$ and $[2\bar{1}\bar{1}0]_\alpha$ is parallel to $[1\bar{1}\bar{1}]_\beta$ [4].

Hot working processes in the $\alpha+\beta$ field (e.g., forging, extrusion, rolling, etc. at temperatures below the beta transus at which beta $\rightarrow$ alpha + beta) comprise the main approaches to breakdown the fully-lamellar microstructure and thus to obtain semi-finished billet and bar products with an equiaxed-alpha microstructure. The design of such processes relies heavily on quantitative descriptions of constitutive behavior and the microstructure changes which underlie plastic-flow behavior.

Accurate modeling of the mechanical behavior of Ti-6Al-4V requires reliable values for different material parameters including the critical resolved shear stress (CRSS) and the subsequent stress-strain response of different slip systems. To this end, there have been a number of efforts to determine the CRSS of different slip systems in Ti-6Al-4V with an equiaxed-alpha microstructure [5, 6, 7, 8]. However, in each case, only the alpha phase of the two phase alloy

was considered, and the beta phase was neglected completely. This approach resulted in large discrepancies in the values of the CRSSs and, consequently, simulations of mechanical behavior.

The early work by Chan, et al. [9] dealing with the room-temperature deformation of Ti-8Al-1Mo-1V represents perhaps the first effort focusing on the deformation response of two-phase titanium alloys with a lamellar (colony-alpha) microstructure. In this research, compression testing of small samples cut from a plate material with a large grain/colony size revealed a marked anisotropy in the critical resolved shear stress for different prism <a>, basal <a>, and pyramidal <c+a> slip systems. Moreover, for a given type of slip system, Schmid's Law failed except for the specific case in which prism slip was activated parallel to the broad face the alpha lamellae (i.e., the alpha-beta interface). A similar anisotropy was reported during the room-temperature deformation of single colonies of Ti 5Al-2.5Sn-0.5Fe oriented for prism slip [10]. In this latter work, TEM was used to correlate the observed anisotropy to the relative orientations of the slip vectors in the alpha and beta phases [4, 10, 11]. In this regard, both Welsch, et al. [11] and Suri, et al. [10] demonstrated that only one of the three <a> slip directions in the alpha phase is closely aligned (within 0.7°) with a <111> slip direction in the beta phase, thus enabling easy slip transmission across the alpha-beta interface. The second <a> slip vector in the alpha phase had a misalignment of ~11.5° with the corresponding <111> slip direction in the β phase, therefore resulting in more difficult slip transmission and a measurably higher critical resolved shear stress. The relative orientation of the third <a> slip vector in the alpha phase was even farther from a <111> slip direction in the beta phase. In follow-on work to that of Suri, et al. [10], Savage, et al. [12] determined the room temperature CRSSs of each of the prism <a> and basal <a> slip systems via micro-tension testing of single colonies of Ti-6242Si (Ti-6Al-2Sn-4Zr-2Mo-0.1Si).

While the limited prior work on single colonies of alpha/beta titanium alloys has provided useful information on deformation behavior at room temperature, there appears to be no comparable single-colony results in the literature at hot working temperatures let alone at any temperature for the most commonly used two-phase alloy, Ti-6Al-4V. Therefore, the current work was undertaken to establish the slip-system anisotropy of the CRSS and stress-strain behavior for all six possible <a> slip systems and the <c+a> pyramidal slip system during hot working of Ti-6Al-4V. For this purpose, single colonies of Ti-6Al-4V were grown using a float-zone technique and subjected to uniaxial hot compression testing.

2. Material and experimental procedure

2.1. Material

Cylindrical Ti-6Al-4V bars containing large alpha/beta colonies were grown utilizing a vertical float-zone technique. The starting material comprised 12-mm diameter bar of Ti-6Al-4V that was supplied by President Titanium, Hanson, MA; it had a measured composition (in weight percent) of 6.33 Al, 4.07 V, 0.19 Fe, 0.16 O, 0.01 C, 0.01 N, 0.0048 H, and balance Ti. Float-zone processing was performed under an argon atmosphere (partial pressure ~ 0.25 atm) in a Crystalox™ furnace. The float zone was produced via RF induction heating using a pancake coil; bars measuring ~400-mm in length were rotated at a rate of 4 RPM and pulled through the hot zone at a speed of 2 mm/h. The colonies so grown ranged in length from 5 mm to 30 mm.

Thin foils parallel to $(0001)_\alpha$ were extracted from one of the rods to determine the precise orientation relationship between the alpha and beta phases via transmission electron microscopy (TEM) in a Philips CM200 LaB_6 microscope (FEI, Hillsboro, Oregon) operated at 200 kV. To avoid the formation of hydride phases normally associated with electropolishing techniques, the

preparation of the TEM samples consisted of dimpling and ion milling in a Pecs Argon Ion mill (made by Gatan Inc., Pleasanton, CA) operated at 5 kV and 40 μA for 6 hours.

2.2. Compression-sample preparation

Seven different colony orientations were chosen for compression testing. Each sample was fabricated to ensure the activation of single slip on the preselected slip system by maximizing the Schmid factor on that system and to verify that the resolved shear stress on each of the other possible slip systems was less than the corresponding CRSS (Table 1). The samples were designated by the corresponding slip plane and slip direction (e.g., prism a_1). The seven IDs were thus denoted as prism a_1, prism a_2, prism a_3, basal a_1, basal a_2, basal a_3, and pyr (c+a) (Fig. 1). Furthermore, prism-slip samples had one face parallel to $(0001)_\alpha$, while basal-slip samples had one face parallel to a $(10\bar{1}0)_\alpha$ plane. Thus, samples oriented for prism slip had the basal plane parallel to the compression axis, thereby preventing slip on the basal plane. Samples aligned for basal slip had one prism plane parallel to the compression axis, therefore preventing slip on that plane. Pyramidal-slip samples had the compression axis perpendicular to the basal plane with a maximum misalignment between the c-axis and the loading direction of 2°. In this case, the loading direction was perpendicular to all three <a> Burgers vectors, essentially eliminating the possibility of prism or basal slip along the close-packed direction.

The fabrication of the single-colony compression specimens (i.e., samples containing a single variant of alpha in a single crystal of beta) began by orienting small sections removed from the float-zone bars. The orientation operation was done using electron-backscatter diffraction (EBSD) in a Leica scanning electron microscope (SEM) (Carl Zeiss SMT Inc., Thornwood, NY) operated at 20 kV and 10 nA. By this means, the crystallographic orientation of the alpha phase was determined simultaneously with the relative alignment of the beta phase,

thus enabling the unambiguous identification of the three <11$\bar{2}$0> slip directions (Fig. 2). To facilitate the orienting process in the SEM, the single-colony sections of the Ti-6Al-4V bars were secured in a special fixture designed to fit inside the column. Subsequent to EBSD, the fixture was removed from the SEM and placed in a wire-EDM (electric-discharge machining) system that ensured minimal loss of sample alignment. A cut parallel to the basal plane in the alpha phase was then made using EDM.

After the basal-plane cut was completed, the orientation of the remaining material was confirmed using an RU300 Laue back-reflection x-ray system (Rigaku, The Woodlands, TX) operated at 40 kV and 200 mA. The resulting Laue patterns were indexed using the OrientExpress™ software [13]. The software was then used to estimate the rotations required to align the desired final sample orientation such that the desired slip-plane normal and slip direction both lay at 45° to the compression axis. The predicted rotations were then applied to the material using standard x-ray goniometers. Last, a Laue pattern was measured again and compared to the prediction for the desired orientation. After fine tuning of the orientation, final EDM cuts were made to produce a compression sample whose shape was a rectangular parallelepiped. Because of the limitation associated with the starting bar diameter and desired sample orientation, each finished specimen was relatively small. Typical sample dimensions were 3 mm x 3 mm x 5 mm with the loading axis aligned with the long side of the sample.

To remove the EDM recast layer and prepare the samples for testing, each specimen was ground flat by hand to a final grit size of 800 and then electropolished for two minutes in a solution of 10 ml perchloric acid and 90 ml methanol at –30°C using a DC power supply operating at 28 volts.

2.3. Test procedures

Uniaxial compression tests were conducted at 815°C using an MTS 810 servo-hydraulic testing machine (MTS Systems Corporation, Eden Prairie, MN) outfitted with induction-heated titanium-carbide tooling. Prior to testing, samples were lubricated with glass ES-14006 (Acheson Colloids Company, Port Huron, MI), which also served to prevent oxidation. Each compression test was conducted at a constant true strain rate of -0.01 s^{-1} to a final axial true strain of -0.15. To measure and control deformation temperatures, thermocouples were welded to the lateral surface of each sample. Immediately after testing, samples were water quenched to retain the as-deformed microstructure.

Following testing, un-sectioned and sectioned samples were prepared for optical and SEM evaluation using standard metallographic procedures. Optical metallography and backscatter-electron (BSE) imaging (in a Leica SEM operated at voltage of 15kV and current of 8 nA) were both utilized to characterize the nature of slip and possible shearing of the alpha platelets and beta matrix.

The measured load-stroke data were corrected for machine compliance and then reduced to resolved shear stress-resolved shear strain by converting first to true axial stress-strain and then applying Schmid's Law ($\tau = \sigma m_s$, in which m_s represents the Schmid factor) and the strain-transformation equation.

3. Results and discussion

The key results of this investigation consisted of characterization of the as-grown single-colony Ti-6Al-4V samples and their flow behavior at 815°C.

3.1. Microstructure and crystallography of single-colony samples

EBSD of the as-grown single-colony samples revealed both the morphology and crystallographic orientation of the alpha platelets (Fig. 2). For example, one of the $<2\bar{1}\bar{1}0>_{\alpha}$

directions in the alpha platelets was indeed nearly parallel to the (broad) alpha-beta interface (inset in Fig. 2a). The corresponding $(0001)_\alpha$, $(11\bar{2}0)_\alpha$, and $(10\bar{1}0)_\alpha$ pole figures further quantified the orientation of each <a> slip direction relative to the sample coordinate system (Fig. 2b).

An overall picture of the morphology of the alpha and beta phases was also revealed in optical micrographs taken on an electropolished sample oriented for prism slip (Fig. 3). The front face of the sample containing the $(0001)_\alpha$ plane (which is parallel to $(101)_\beta$ plane) showed the alpha phase as thin platelets separated by interlayers of the beta matrix (Fig. 3). The side and top faces of the sample revealed the finite breadth and length of the alpha platelets. The volume fraction of the alpha phase was ~0.90, and the average alpha-platelet thickness was ~ 8.5 μm (Fig. 2a). The beta interlayers were ~ 1-μm thick.

The orientation relationship (OR) between the alpha and beta phases in Ti-6Al-4V with a lamellar-alpha microstructure was revealed by TEM for imaging conditions in which the electron beam was parallel to $(0001)_\alpha \| (101)_\beta$ (Fig. 4a). Convergent-beam electron diffraction (CBED) patterns for both phases were superimposed on the bright-field (BF) TEM image with $[0001]_\alpha$ and $[101]_\beta$ zone axes (Fig. 4a). An analysis of the TEM images indicated that the OR between the alpha and beta phases in Ti-6Al-4V was indeed near that prescribed by the Burgers orientation relationship and was in agreement with prior work for near-alpha titanium alloys [10, 12, 14].

Based on previous work, the OR was expected to result in one of the <a> slip directions in the hcp alpha phase ($a_1 \sim [2\bar{1}\bar{1}0]_\alpha$) being parallel to one of the <111> slip directions in the bcc beta phase ($b_1 \sim [1\bar{1}\bar{1}]_\beta$) (Fig. 4b). A careful examination of the SAD patterns revealed a slight misalignment of 0.8° about the $(0001)_\alpha \| (101)_\beta$ zone axes between the a_1 slip direction in

the alpha phase and the b_1 slip direction in the beta phase (Fig. 4b). The a_2 slip direction in the alpha phase was misoriented by approximately 11.2° from the b_2 slip direction in the beta phase. The a_3 slip direction in the alpha phase was not close to any of the close-packed directions in the beta phase.

The relative inclination of the different slip directions to the alpha-beta interface was determined by overlapping the SAD patterns with the BF TEM image with $[0001]_\alpha$ and $[101]_\beta$ zone axes (Fig. 5). The measured inclinations of the a_1, a_2, and a_3 slip directions to the alpha-beta interface were 14.5°, 74.5°, and 45.5°, respectively.

3.2. Flow behavior

The flow behavior in terms of the resolved shear stress – strain plots revealed a number of interesting features for the samples cut to produce prism <a>, basal <a>, or pyramidal <c+a> slip.

3.2.1. Prism <a> deformation

Constant strain rate, resolved shear stress-strain data for the Ti-6Al-4V single-colony samples oriented for *prism* slip showed a significant anisotropy in both initial strength (~yield strength/CRSS) and subsequent strain-hardening behavior (Figure 6). The CRSSs (calculated from the 0.2% proof stress) for the prism a_2 and a_3 systems were ~ 42%. or 76%. higher, respectively, than that for prism a_1 slip. The different systems also exhibited different degrees of flow softening at large strains.

The anisotropy in the prism-slip mechanical behavior can be rationalized in the context of slip transmission across alpha-beta interfaces. For prism a_1 slip, for example, the slip vector in the alpha phase is closely aligned with a <111> slip direction in the beta phase phase. Consequently, dislocations can be transferred across the alpha-beta interface with minimum

resistance [10, 12]. By contrast, a very high resistance for slip transmission across the interface was encountered by dislocations gliding on the a_3 system during testing of the corresponding prism sample because there was no closely-aligned <111> slip direction in the beta phase. Consequently, the alpha-beta interface acted as a strong barrier to dislocation movement and increased the yield strength of the material. The small misalignment between the a_2 and b_2 directions (11.2°) resulted in a yield strength intermediate between those for the soft a_1 and hard a_2 prism slip systems. A similar behavior has been reported during the *room-temperature* testing of near-alpha titanium alloys [9, 10, 12]. In particular, the observations for colonies 22 and 3 in the work by Chan, et al. [9], colonies OA and OB in the work of Suri, et al. [10], and the prism a_1 and a_2 samples in the work of Savage, et al. [12] mirror the present results, even though the current tests were conducted at 815°C.

Despite the similarity in the relative flow stress of the prism systems at high temperature (present work) and room temperature (prior work), the large-strain behavior did show some noticeable differences. At room temperature, plastic flow at finite strains was characterized by strain-hardening to a strain of 0.08. At 815°C, on the other hand, the deformation of the easy-slip prism system (a_1) exhibited an initial strain-hardening transient followed by steady-state flow. Furthermore, the prism a_2 and a_3 systems showed marked or modest flow softening, respectively, following the initial strain hardening transient at 815°C. These latter behaviors may be ascribed to the difficulty of slip transmission when there are no co-linear slip vectors in the alpha and beta phases. Hence, as deduced for the hot working of poly-colony samples by Semiatin and Bieler [15], the higher initial flow stresses and flow softening for the prism a_2 and a_3 systems are likely due to a Hall-Petch (H-P) like effect for the peak stress and the gradual loss of the H-P effect due to slip transmission at higher strains, respectively. The magnitude of the H-P contribution to the

peak stress (at low strains) would depend of course on the inverse square-root slip length and the magnitude of the H-P constant. For a given alpha-platelet thickness, the slip-length contribution is greater for the a_3 system because its slip plane lies at a less shallow angle to the interface (~75°) than the a_2 system (~45°). However, the difference in inverse square-root slip length for the a_2 and a_3 slip systems for the present material (with relatively thick alpha plates) would be small (~14%). Thus, the major contribution to the difference in the peak stresses for prism a_2 and a_3 deformation was most likely related to the difference in H-P constants and the detailed nature of slip transfer in the two different cases.

Despite the hypothesis that slip transfer between the alpha and beta phases is inherently easy for the prism a_1 system and the fact that flow softening suggests slip transfer and the associated loss of H-P hardening for the a_2 and a_3 systems, metallography revealed no evidence of distinct slip steps following compression at 815°C. Specifically, numerous BSE SEM images did not reveal any shearing of the alpha-beta interfaces in deformed samples (Fig. 7) in contrast to the previous findings for room-temperature testing [10, 12].

There are several possible explanations for the absence of slip steps in the present work. First, flow-localization calculations [16] suggest that the amount of strain concentration (leading to shear bands/slip offsets) is very low for deformations of the order of those imposed in the present work and strain-rate sensitivities typical of hot working at 815°C and a strain rate of 0.01 s^{-1} (i.e., m ~ 0.15). In a similar vein, it has been shown that strains of the order of unity are required to *begin* dynamic spheroidization (due to platelet shearing) in Ti-6Al-4V with a polycolony microstructure containing coarse alpha plates [17]. The high strain-rate sensitivity at hot-working temperatures contrasts with an m value which is very small at room temperature (m ~ 0). Hence, the strain localization process in the presence of a small thickness non-uniformity

would be expected to occur very quickly (i.e., at rather low strains) at ambient temperature, as has been observed by Suri, et al. [10].

In addition to the flow-localization argument, a small amount of migration of the alpha-beta interface during cool-down (due to the increase in alpha volume fraction with decreasing temperature) might have occurred despite the fact that the samples were water quenched after deformation. Such migration may have eliminated the interface roughness associated with slip transfer. Finally, the high deformation temperature and coarse alpha-plate thickness present in the float-zone samples may have allowed dislocation climb, dynamic recovery, and the formation of subgrains, thus minimizing the formation of the dislocation pile-ups that precede slip transmission.

3.2.2. Basal <a> and pyramidal <c+a> deformation

The mechanical behavior of samples oriented for basal <a> slip also showed a noticeable anisotropy (Fig. 8). However, the flow stress of the basal a_1 system was ~35% *higher* than that for the basal a_3 system. Although the higher flow stress of basal a_1 compared to basal a_3 contrasts with the corresponding high-temperature observations for prism slip, the trend is very similar to that seen previously by Savage, et al. [12] for room-temperature deformation via micro-tension testing. On the other hand, the room-temperature *compression* results of Savage, et al. [18] did indeed show that the flow stress for basal a_1 slip was less than that for basal a_3 slip. Nevertheless, the room-temperature compression flow behavior of the basal a_2 system was close to that for basal a_3 which is similar to the findings in the current work (Figure 8).

Samples compressed parallel to the c-axis of the alpha phase showed the highest flow stress of all (Figs. 9, 10). In particular, the initial stress for <c+a> slip was more than twice that for the activation of prism a_1 slip, the softest system for Ti-6Al-4V.

4. Summary and conclusions

A float-zone technique was used to produce Ti-6Al-4V bars with large lamellar colonies from which small single-colony compression samples were extracted. The alpha lamellae exhibited a classical Burgers orientation relation with the beta matrix. Constant strain-rate compression testing of the single colony samples at 815°C revealed a distinct anisotropy in plastic-flow behavior. From this work, the following conclusions were drawn:

(1) The CRSS for prism slip is lowest along the along a_1 direction and highest along the a_3 direction. The reverse is true for basal slip. The pyramidal <c+a> slip system had the highest CRSS of all. These trends are analogous to previous room-temperature observations for near-alpha titanium alloys with a lamellar microstructure.

(2) Flow softening to various degrees was observed for all slip systems tested. It was most pronounced for pyramidal slip.

(3) Shearing of beta lamellae due to slip transmission was not observed during high temperature deformation. This may be due to the small strains imposed and the sluggish kinetics of strain localization associated with high m values that characterize high-temperature plastic flow.

Acknowledgments

This work was conducted as part of the in-house research activities of the Metals Processing Group of the Air Force Research Laboratory's Materials and Manufacturing Directorate. The support and encouragement of the Laboratory management and the Air Force Office of Scientific Research (Dr. J. Fuller, program manager) are gratefully acknowledged. The yeoman assistance of J.M. Scott, P.N. Fagin, and F. Meisenkothen in conducting the experimental work is much appreciated. One of the authors (AAS) was supported through Air Force Contract F33615-03-D-5801.

References

1. D. Eylon, S.R. Seagle, in: *Titanium 99: Science and Technology*, ed. I.V. Gorynin, and S.S. Ushkov, CRISM "PROMETEY", St. Petersburg, 2000, pp. 37-41
2. S.L. Semiatin, V. Seetharaman and I. Weiss, in: *Advances in the Science and Technology of Titanium Alloy Processing*, TMS, Warrendale, PA, 1997, pp. 3-73.
3. G. Lutjering, *Materials Science and Engineering* A243 (1998) 32-45.
4. W.G. Burgers, *Physica* 1 (1934) 561-586.
5. M.J. Philippe, M. Serghat, P. Van Houtte, and C. Esling, *Acta Metal and Mater.* 43 (1995) 1619-1630.
6. J.A. Medina Perllia, and J. Gil Sevillano, *Mater. Sci. Eng.* A201 (1995) 103-110.
7. J.J. Fundenberger, M.J. Philippe, F. Wagner, and C. Esling, *Acta Mater.* 45 (1997) 4041-4055.
8. T. Dick and G. Cailletaud, *Computational Materials Science* 38 (2006) 113-125.
9. K.S. Chan, C.C. Wojcik, and D.A. Koss, *Metall. Trans.* 12A (1981) 1899-1907.
10. S. Suri, G.B. Viswasnathan, T. Neeraj, D.-H. Hou, and M.J. Mills, *Acta Mater.* 47 (1999) 1019-1034.
11. G. Welsch, I. Weiss, D. Eylon, and F.H. Froes in: *Advances in the Science and Technology of Titanium Alloy Processing*, TMS, Warrendale, PA, 1997, pp. 169-183.
12. M.F. Savage, J. Tatalovich, M. Zupan, K.J. Hemker, and M.J. Mills, *Mat. Sci. and Eng.* A319–321 (2001) 398–403.
13. J. Laugier, and B. Bochu, *LMGP Suite of Programs for the interpretation of X-ray Experiments*, ENSP/Laboratoire des Matériaux et du Génie Physique, Saint Martin d'Hères, France (1999).

14. M.J. Mills, D.H. Hou, S. Suri, and G.B. Viswanathan, in: *Boundaries and Interfaces in Materials*, TMS, Warrendale, PA, 1998, pp. 295-301.
15. S.L. Semiatin and T.R. Bieler, *Acta Mater.* 49 (2001) 3565-3573.
16. S.L. Semiatin, Unpublished research, Air Force Research Laboratory, Wright-Patterson Air Force Base, OH (2000).
17. E.B. Shell and S.L. Semiatin, *Metall. and Mater. Trans.* 30A (1999) 3219-3229.
18. M.F. Savage, J. Tatalovich, and M.J. Mills, *Phil. Mag.* 84 (2004) 1127–1154.

Table 1. Calculated Schmid factors and resolved shear stresses for different slip systems in single colonies of Ti-6Al-4V. The primary slip systems are shaded in gray.

Sample ID	Slip Systems in α Phase	Schmid Factors in α Phase	Resolved Shear Stress (MPa)
Prism a_1	a_1 prismatic	0.47	43
	a_2,a_3 prismatic	0.3, 0.18	27, 16
	a_1,a_2,a_3 basal	0.07, 0.09, 0.01	6, 8, 1
Prism a_2	a_2 prismatic	0.49	61
	a_1,a_3 prismatic	0.13, 0.34	16, 42
	a_1,a_2,a_3 basal	0	0
Prism a_3	a_3 prismatic	0.50	81
	a_1, a_2 prismatic	0.19, 0.33	31, 54
	a_1, a_2, a_3 basal	0	0
Basal a_1	a_1 basal	0.48	73
	a_2,a_3 basal	0.15, 0.12	23, 18
	a_1,a_2,a_3 prismatic	0.04, 0.25, 0.2	6, 38, 30
Basal a_2	a_2 basal	0.50	61
	a_1, a_3 basal	0.24, 0.24	29, 28
	a_1,a_2, a_3 prismatic	0.23, 0.04, 0.23	28, 5, 28
Basal a_3	a_3 basal	0.47	54
	a_1,a_2 basal	0.15, 0.33	17, 38
	a_1,a_2,a_3 prismatic	0.14, 0.23, 0.09	16, 26, 10
Pyr (c+a)	c+a pyramidal	0.4	119
	a_1,a_2,a_3 prismatic	0	0
	a_1,a_2,a_3 basal	0	0

Figure Captions

Fig. 1. Schematic illustration showing the relative orientation of the compression axis and the various slip systems in the present work: (a-c) prism <a> slip, (d-f) basal <a> slip, and (g) pyramidal <c+a> slip. The double line in a-c represents beta lamellae.

Fig. 2. (a) EBSD inverse-pole-figure map for an as-grown single-colony sample (inset shows the orientation of the alpha unit cell) and (b) pole figures for this sample.

Fig. 3. Optical micrograph showing the morphology of a single colony of Ti-6Al-4V oriented for prism <a> slip: (a) the front face of the sample is $(0001)_\alpha \| (101)_\beta$, (b) the top face (compression plane), and (c) the side face. The compression axis is vertical.

Fig. 4. (a) Bright-field TEM image at the alpha-beta interface of a single-colony sample showing the adjacent beta and alpha lamellae. The insets are convergent-beam electron-diffraction patterns from the alpha and beta phases using $[0001]_\alpha$ and $[101]_\beta$ zone axes. (b) Selected-area diffraction pattern taken at the alpha-beta interface along the $[0001]_\alpha \| [101]_\beta$ direction revealing the relative alignment of the hcp (alpha-phase) a_1, a_2, and a_3 directions with bcc (beta) b_1 and b_2 directions confirming the near-Burgers relation between the alpha and beta phases.

Fig. 5. Bright field TEM micrograph and corresponding schematic drawing overlapped with the SAD results (with the beam direction parallel to $[0001]_\alpha \| [101]_\beta$) showing the relative inclination of the three <a> directions relative to the alpha-beta interface.

Fig. 6. Resolved shear stress-strain curves for Ti-6Al-4V single-colony specimens oriented to activate the prism a_1, a_2, or a_3 slip systems during compression at 815°C.

Figure 7. Backscattered-electron SEM image for a prism a_1 sample after compression at 815°C to a true strain of 0.12 followed by water quenching. No interface shearing was observed in the sample.

Fig. 8. Resolved shear stress-strain curves for Ti-6Al-4V single-colony specimens oriented to activate the basal a_1, a_2, or a_3 slip systems during compression at 815°C.

Fig. 9. Comparison of the resolved shear stress-strain curves for Ti-6Al-4V single-colony samples oriented to activate the pyramidal <c+a>, basal a_1, or prism a_1 slip system during compression at 815°C.

Fig. 10. Comparison of all of the critical resolved shear stress (CRSS) data for basal <a>, prism <a>, and pyramidal <c+a> slip systems at 815°C.

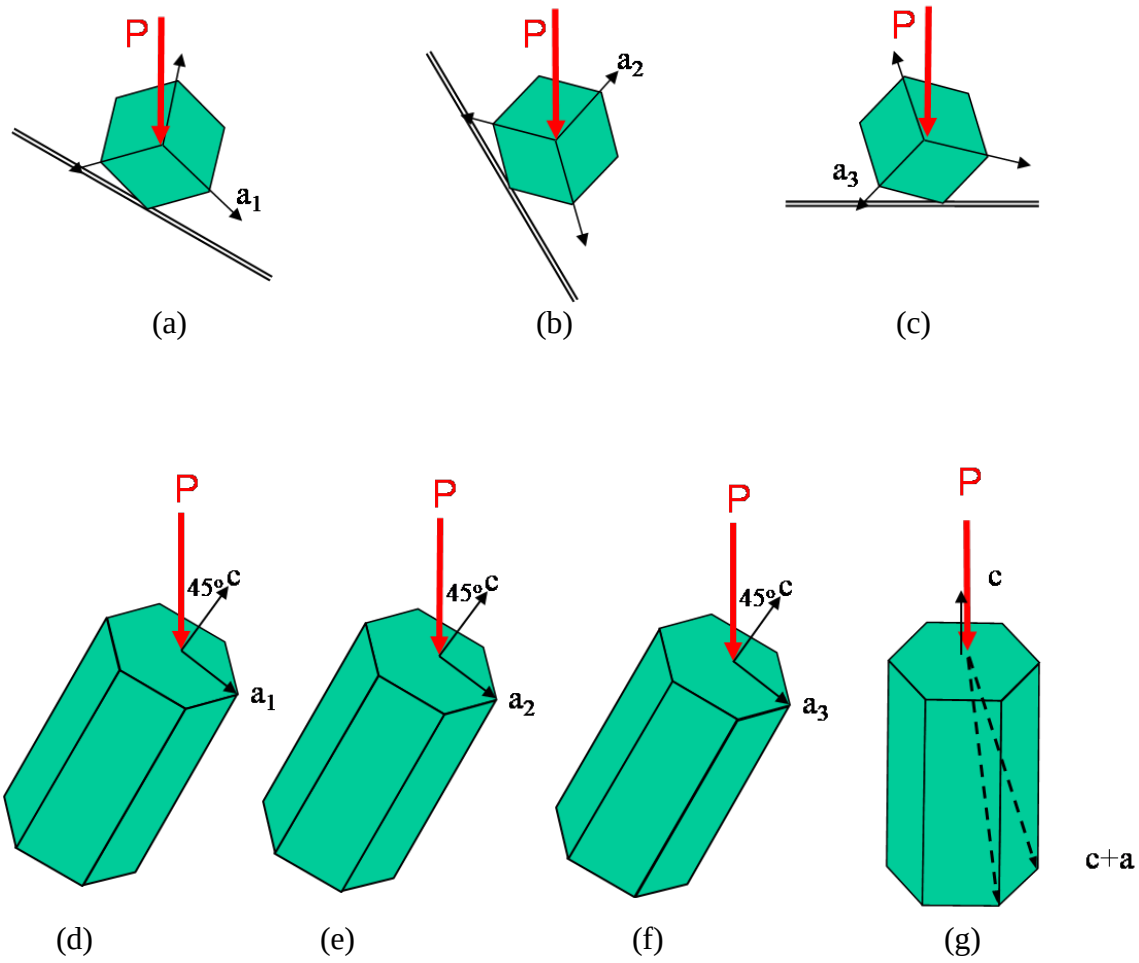

Fig. 1. Schematic illustration showing the relative orientation of the compression axis and the various slip systems in the present work: (a-c) prism <a> slip, (d-f) basal <a> slip, and (g) pyramidal <c+a> slip. The double line in a-c represents beta lamellae.

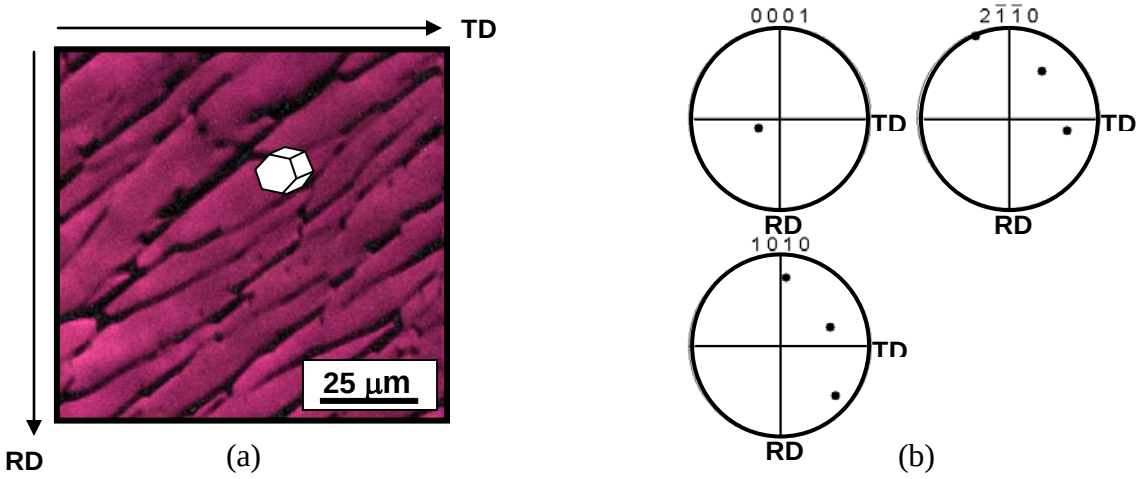

Fig. 2. (a) EBSD inverse-pole-figure map for an as-grown single-colony sample (inset shows the orientation of the alpha unit cell) and (b) pole figures for this sample.

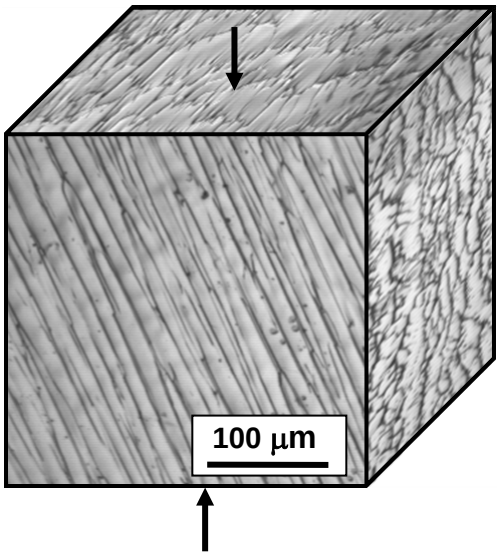

Fig. 3. Optical micrograph showing the morphology of a single colony of Ti-6Al-4V oriented for prism <a> slip. The front face of the sample is $(0001)_\alpha \parallel (101)_\beta$. The top face is the compression plane.

(a) (b)

Fig. 4. (a) Bright-field TEM image at the alpha-beta interface of a single-colony sample showing the adjacent beta and alpha lamellae. The insets are convergent-beam electron-diffraction patterns from the alpha and beta phases using $[0001]_\alpha$ and $[101]_\beta$ zone axes. (b) Selected-area diffraction pattern taken at the alpha-beta interface along the $[0001]_\alpha \| [101]_\beta$ direction revealing the relative alignment of the hcp (alpha-phase) a_1, a_2, and a_3 directions with bcc (beta) b_1 and b_2 directions confirming the near-Burgers relation between the alpha and beta phases.

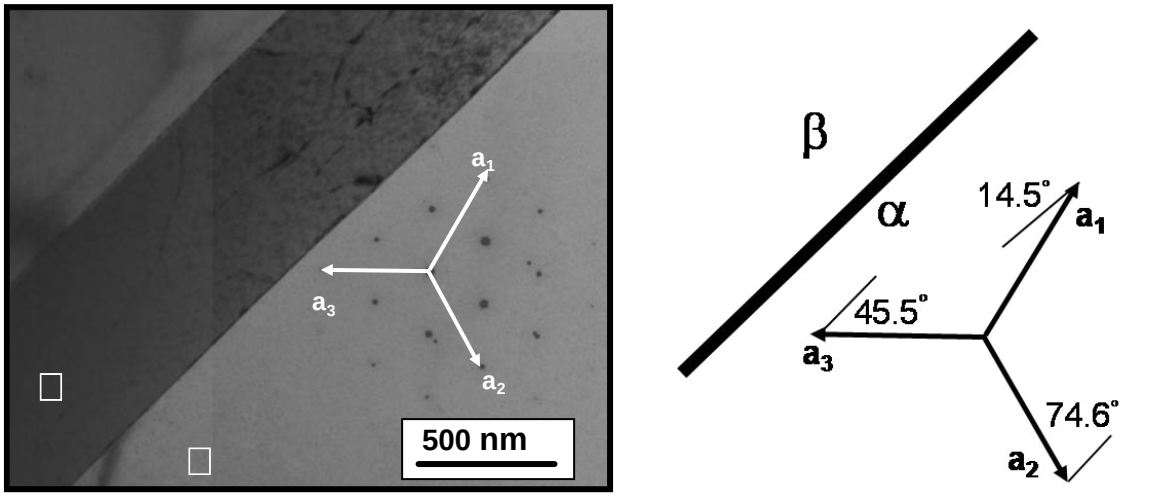

(a) (b)

Fig. 5. Bright field TEM micrograph and corresponding schematic drawing overlapped with the SAD results (with the beam direction parallel to $[0001]_\alpha \| [101]_\beta$) showing the relative inclination of the three <a> directions relative to the alpha-beta interface.

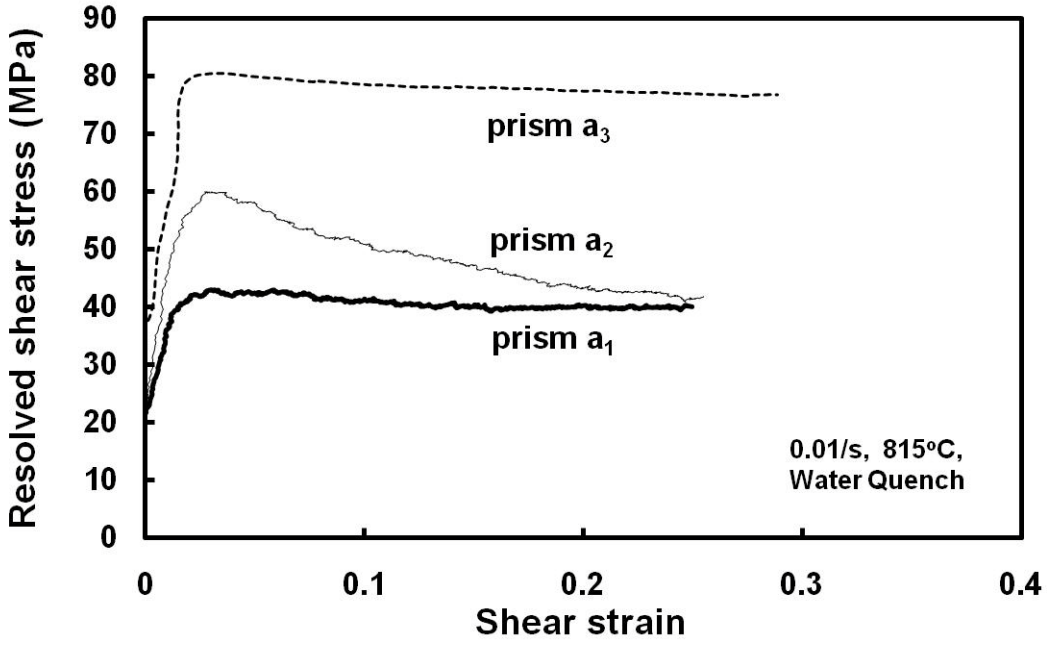

Fig. 6. Resolved shear stress-strain curves for Ti-6Al-4V single-colony specimens oriented to activate the prism a_1, a_2, or a_3 slip systems during compression at 815°C.

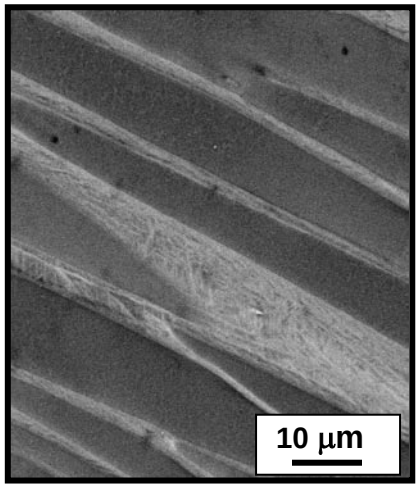

Figure 7. Backscatter-electron SEM image for a prism a_1 sample after compression at 815°C to a true strain of 0.12 followed by water quenching. No interface shearing was observed in the sample.

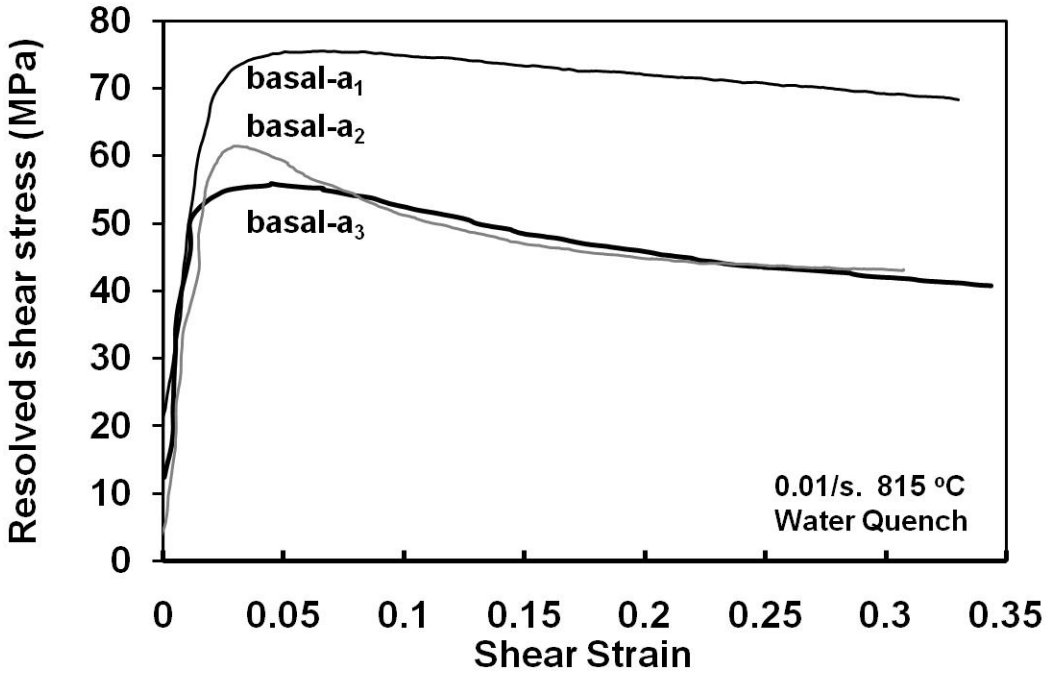

Fig. 8. Resolved shear stress-strain curves for Ti-6Al-4V single-colony specimens oriented to activate the basal a_1, a_2, or a_3 slip systems during compression at 815°C.

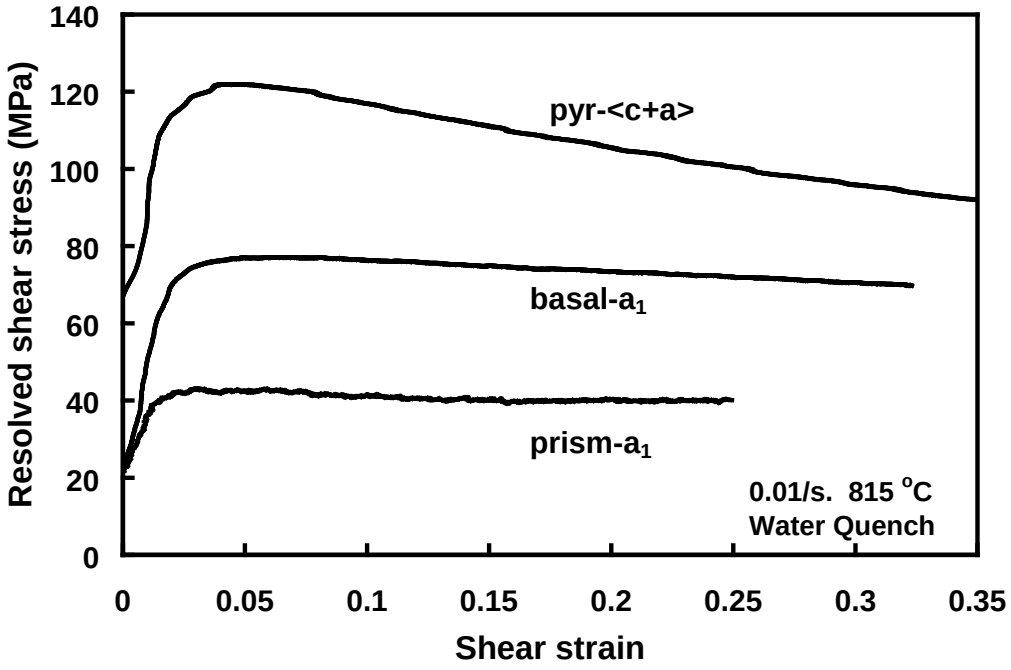

Fig. 9. Comparison of the resolved shear stress-strain curves for Ti-6Al-4V single-colony samples oriented to activate the pyramidal <c+a>, basal a_1, or prism a_1 slip system during compression at 815°C.

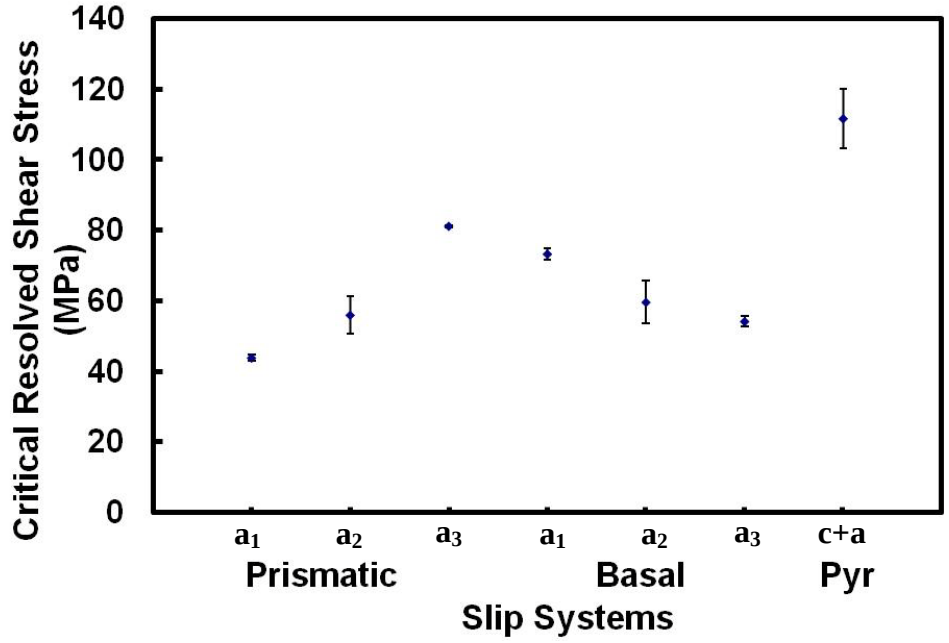

Fig. 10. Comparison of all of the critical resolved shear stress (CRSS) data for basal <a>, prism <a>, and pyramidal <c+a> slip systems at 815°C.